

2002

## Increasing Proton Exchange Membrane Fuel Cell Catalyst Effectiveness Through Sputter Deposition

Andrew T. Haug

*University of South Carolina - Columbia*

Ralph E. White

*University of South Carolina - Columbia, white@cec.sc.edu*

John W. Weidner

*University of South Carolina - Columbia, weidner@engr.sc.edu*

Wayne Huang

Steven Shi

*See next page for additional authors*

Follow this and additional works at: [https://scholarcommons.sc.edu/eche\\_facpub](https://scholarcommons.sc.edu/eche_facpub)



Part of the [Chemical Engineering Commons](#)

---

### Publication Info

*Journal of the Electrochemical Society*, 2002, pages A280-A287.

© The Electrochemical Society, Inc. 2002. All rights reserved. Except as provided under U.S. copyright law, this work may not be reproduced, resold, distributed, or modified without the express permission of The Electrochemical Society (ECS). The archival version of this work was published in the *Journal of the Electrochemical Society*.

<http://www.electrochem.org/>

Publisher's link: <http://dx.doi.org/10.1149/1.1446082>

DOI: 10.1149/1.1446082

This Article is brought to you by the Chemical Engineering, Department of at Scholar Commons. It has been accepted for inclusion in Faculty Publications by an authorized administrator of Scholar Commons. For more information, please contact [digres@mailbox.sc.edu](mailto:digres@mailbox.sc.edu).

---

**Author(s)**

Andrew T. Haug, Ralph E. White, John W. Weidner, Wayne Huang, Steven Shi, Timothy Stoner, and Narender Rana



## Increasing Proton Exchange Membrane Fuel Cell Catalyst Effectiveness Through Sputter Deposition

Andrew T. Haug,<sup>a,\*</sup> Ralph E. White,<sup>a,\*\*</sup> John W. Weidner,<sup>a,\*\*\*,z</sup> Wayne Huang,<sup>b</sup> Steven Shi,<sup>b,\*\*\*</sup> Timothy Stoner,<sup>c</sup> and Narender Rana<sup>c</sup>

<sup>a</sup>Center for Electrochemical Engineering, Department of Chemical Engineering, University of South Carolina, Columbia, South Carolina 29208, USA

<sup>b</sup>Plug Power, Incorporated, Latham, New York 12110, USA

<sup>c</sup>New York State Fuel Cell Institute, Center for Advanced Thin Film Technology, Albany, New York 12203, USA

Sputter deposition has been investigated as a tool for manufacturing proton-exchange membrane fuel cell (PEMFC) electrodes with improved performance and catalyst utilization vs. ink-based electrodes. Sputter-depositing a single layer of Pt on the gas diffusion layer provided better performance (0.28 A/cm<sup>2</sup> at 0.6 V) than sputtering the Pt directly onto a Nafion membrane (0.065 A/cm<sup>2</sup> at 0.6 V) and equaled the performance of the baseline for an equivalent Pt loading. Sputter-depositing alternating layers of Pt and Nafion-carbon ink (NCI) onto the membrane did not increase the performance over the baseline as measured in amperes per centimeter squared due to the excessive thickness of the NCI (the NCI accounted for 99.9% of the electrode thickness). However, three and six layer Pt/NCI membrane electrode assemblies (MEAs) resulted in Pt activities double that of the 905 A/g at 0.6 V achieved by the ink-based baseline. Decreasing the thickness of each NCI layer increased the performance of the six-layered Pt/NCI MEA from 0.132 to 0.170 A/cm<sup>2</sup> at 0.6 V, providing an activity of 2650 A/g at 0.6 V. It is likely that by further decreasing the ratio of NCI to Pt in these electrodes, Pt activity, and PEMFC electrode performance can be increased.

© 2002 The Electrochemical Society. [DOI: 10.1149/1.1446082] All rights reserved.

Manuscript submitted July 11, 2001; revised manuscript received October 5, 2001. Available electronically January 29, 2002.

Proton exchange membrane fuel cells (PEMFCs) are gaining popularity due to their high operating efficiency and environmental friendliness. One of the barriers to commercialization is the prohibitive cost of this technology.<sup>1</sup> In a recent solicitation, the U.S. Department of Energy set long-term goals for PEMFC performance in a 50 kW stack that included operation with cathode loadings of 0.05 mg/cm<sup>2</sup> or less of precious metals.<sup>2</sup>

Typical methods of manufacturing membrane-electrode assemblies (MEAs) for PEMFCs involve painting, spraying, or printing of catalyst inks that contain a matrix of electrolyte and carbon-supported catalyst.<sup>3-6</sup> It is this three-phase interface of catalyst, carbon, and electrolyte (typically Nafion<sup>®</sup>) that allows effective gas and water diffusion and proton transport and electron transport to and from the catalyst sites. Refinements of this process have involved optimizing the ratios of Pt, C, and Nafion present in this three-phase interface.<sup>3,5</sup> There are limitations on the catalyst activity imposed by the particle size of Pt on activated carbon.

As alternatives, electrodeposition and sputter deposition have been used to manufacture MEAs of low catalyst loadings.<sup>3,7-14</sup> Both pulse and direct current (dc) electrodeposition have been used to localize a thin layer of Pt near the surface of the MEA,<sup>7,8</sup> resulting in the development of electrodes on the order of 0.05 mg Pt/cm<sup>2</sup>.<sup>8</sup> Sputter deposition is widely used for integrated circuit manufacturing and has been investigated for the preparation of more effective fuel cell electrodes for more than a decade. Srinivasan *et al.*<sup>3,9-11</sup> applied a 50 nm Pt-sputtered film to the front surface of a catalyzed gas diffusion layer (GDL) to reduce the loading tenfold (4 mg/cm<sup>2</sup> to 0.4 mg Pt/cm<sup>2</sup>) without reduction in performance. Hirano *et al.*<sup>12</sup> sputter deposited platinum on uncatalyzed GDLs resulting in cell performances at loadings of 0.10 mg Pt/cm<sup>2</sup> equivalent to those of standard methods at loadings of 0.40 mg Pt/cm<sup>2</sup>. Sputter deposition has been used to reduce the amount of anode catalyst required for direct methanol fuel cell (DMFC) anodes as well. Witham *et al.*<sup>13</sup> achieved DMFC anode catalyst activities one to two orders of magnitude higher than those of conventional ink-based catalysts, sug-

gesting that DMFC anodes could be manufactured containing less than one-tenth the amounts presently used (2.5-4 mg Pt/cm<sup>2</sup>) without loss in performance.

Cha and Lee<sup>14</sup> alternated sputtering microthin (5 nm) Pt layers and painting layers of Nafion and carbon ink directly onto the membrane. By reducing the amount of Pt on each layer, they were able to achieve cell performances at extremely low loadings (~0.043 mg/cm<sup>2</sup>) that were nearly equivalent to that of higher loadings (~0.5 mg/cm<sup>2</sup>) under similar conditions. Very efficient usage of Pt is demonstrated in this method.

The goal of this work was to examine the sputter-deposition technique as a means to improve performance and/or reduce the catalyst loading of proton exchange membrane (PEM) fuel cells. First Pt was sputtered on the different substrates that comprise individual fuel cells. These were built into MEAs and compared to MEAs made through ink-based methods and ink-based MEAs augmented through sputter deposition. Based on these results, GDLs and membranes were then subjected to the layered technique first developed by Cha and Lee<sup>14</sup> with the goal of reducing the amount of Pt catalyst used and increasing fuel cell performance. Based upon the findings, improvements were made on Cha and Lee's technique allowing for the manufacture of thinner, more effective electrodes for MEAs.

### Experimental

**Catalyst inks.**—The method for the catalyst ink preparation and MEA fabrication performed in this project have been described elsewhere.<sup>4</sup> The following catalyst inks were prepared: (i) Nafion + carbon only (Nafion-carbon ink or NCI) and (ii) Nafion + 20% Pt on carbon.

The inks were prepared for Pt by adding the E-TEK catalyst (20% catalyst on XC-72 carbon) to a solution of 5 wt % Nafion (DuPont). In the case of NCI, XC-72 carbon was added to a solution of 5 wt % Nafion.

**Ink-based MEAs.**—Decals (Teflon, 10 cm<sup>2</sup>, three ply) were weighed prior to application of the catalyst ink. The ink was drawn across the surface of the decals using a Meyer rod. Anode and cathode target loadings for the baseline ink-based MEA were both 0.15 mg Pt/cm<sup>2</sup> for a combined MEA loading of 0.30 mg Pt/cm<sup>2</sup>. A low Pt loading was chosen as the baseline because low catalyst loading is a goal for commercializing PEMFCs.<sup>2</sup> The coated decals were dried in an oven at 105°C under ambient pressure for 10 min.

\* Electrochemical Society Student Member.

\*\* Electrochemical Society Fellow.

\*\*\* Electrochemical Society Active Member.

<sup>z</sup> E-mail: weidner@engr.sc.edu

To form a MEA with ink-coated decals, appropriate decals were placed on either side of the PEM (Nafion 117, protonated form). This assembly was hot-pressed to ensure bonding. It was then cooled to room temperature, before the decals were carefully peeled from the assembly. An uncatalyzed gas diffusion layer (Toray) was placed on either side of the MEA to complete the membrane-electrode unit (MEU).

**Plasma treatment and Pt sputter deposition.**—Nafion 117 membranes, uncatalyzed GDLs (Toray) and MEAs were chosen as substrates for sputter deposition. Plasma modifications and sputter-deposition augmentations/additions were both completed using an Anatech Hummer 10.2 sputter-coating tool. A modified sample stage was used to support PEM, MEA, and GDL substrates of sizes up to  $6 \times 6$  cm while masking 1.5 cm about the membrane's perimeter. An aluminum target was used for ac and dc plasma modifications, while the Pt (Anatech) targets as well as a carbon evaporation system (Anatech) were used for sputter-deposition augmentations/additions.

All PEMs, MEAs, and GDLs subject to sputter-deposition were first ac plasma cleaned for a period of 5 min at 5 mA and 1.2 kV to remove residual buildup from the target as well as roughen the substrate surface. All treatments were completed at a pressure of  $\sim 62$  mTorr. A separate vacuum chamber was used to evacuate each substrate to a pressure of  $\sim 45$  mTorr, before it was placed in the sputter-coating tool to minimize contaminant out-gassing in the deposition chamber.<sup>15</sup>

Since all plasma and sputter-deposition treatments must be performed under vacuum, the stability of Nafion 117 under vacuum was evaluated. Each PEM material was slowly evacuated to a pressure below 1 mTorr. Nafion 117 remained very pliable following evacuation. Mass measurement of Nafion before and after seven different evacuation and processing sequences indicated that the membrane loses approximately 2.3% of its total mass as a result of dehydration during evacuation. In each case however, Nafion quickly ( $\sim 30$  min) rehydrates upon exposure to ambient air. The exposed membranes were then built into MEAs and subjected to performance testing. They performed analogously to nonevacuated membranes, indicating that Nafion was a viable candidate for plasma and sputter-deposition treatments. The performance of a vacuum-treated MEA also showed no adverse effects when tested.

A potential of 1.8 kV and a current of 8 mA was maintained to control the deposition rate for Pt. A  $\text{SiO}_2$  sample was sputter-deposited *in situ* with each PEM, MEA, or GDL. The resultant metal/ $\text{SiO}_2$  stack was subjected to cross-sectional view SEM imaging to verify the sputter-deposited film thickness and top-view SEM imaging to determine surface characteristics of the film.

Multilayered MEAs were prepared by first spraying the anode and cathode sides of PEM with NCI. The MEA was then subject to a vacuum of 30 mTorr before the appropriate catalyst was sputter deposited. This sequence was repeated until the desired number of layers was achieved. Multilayered GDLs were prepared by an identical process except that only one side of the GDL was treated.

MEAs containing sputter-deposited catalyst layers were built into MEUs through methods similar to that of the baseline. In the case of multilayered GDLs, appropriate GDLs were placed on either side of a blank Nafion 117 membrane and hot-pressed to ensure a well-bonded MEU.

**Cell assembly and testing.**—The MEUs were placed in a  $10 \text{ cm}^2$  cell assembly and incubated for 4 to 8 h at ambient pressure, cell temperature of  $70^\circ\text{C}$ , stoichiometric ratio ([actual flow]/[stoichiometric flow] required for a  $1.0 \text{ A/cm}^2$  current) of 1.5 at the anode and 2.0 at the cathode. Fuel cell performance curves were obtained under the conditions set out in Table I.

## Results

**AC and dc plasma roughening.**—The AFM images in Fig. 1 show the effects of an ac plasma treatment on Nafion. Both ac

**Table I. Fuel cell test conditions.**

Pressure	1 atm
Cell temperature	$70^\circ\text{C}$
Stoichiometric ratio (at $1 \text{ A/cm}^2$ )	1.5 Hydrogen 2.0 Air
Feedstreams	Anode: hydrogen Cathode: air
Humidification	Complete humidification of anode and cathode gas streams for all trials.

plasma and dc plasma substantially roughen the surface of the PEM. Analogous roughening by ac plasma or dc plasma did not significantly increase the surface of MEAs or GDLs, since the surfaces of these samples are much rougher in their original state. The SEM images in Fig. 2 document the influence of ac and dc plasma modification of MEAs. The high and medium magnification SEM images both suggest ac and dc plasma minimally alter the surface of the MEA. However, the low magnification SEM images indicate that dc plasma treatments create cracks in the surface layer of the MEAs. Therefore, ac plasma treatments were used throughout the remainder of this program. It was hoped that roughening the surface of the PEM or MEA would enhance fuel cell performance by increasing the number of active catalytic sites. However, performance of MEUs made from roughened PEMs and MEAs showed no improvement over a baseline MEU.

**Determination of sputter-deposition rates and catalyst loading.**—The top view SEM images in Fig. 3 were analyzed to determine the surface coverage of the sputter-deposited film (Pt

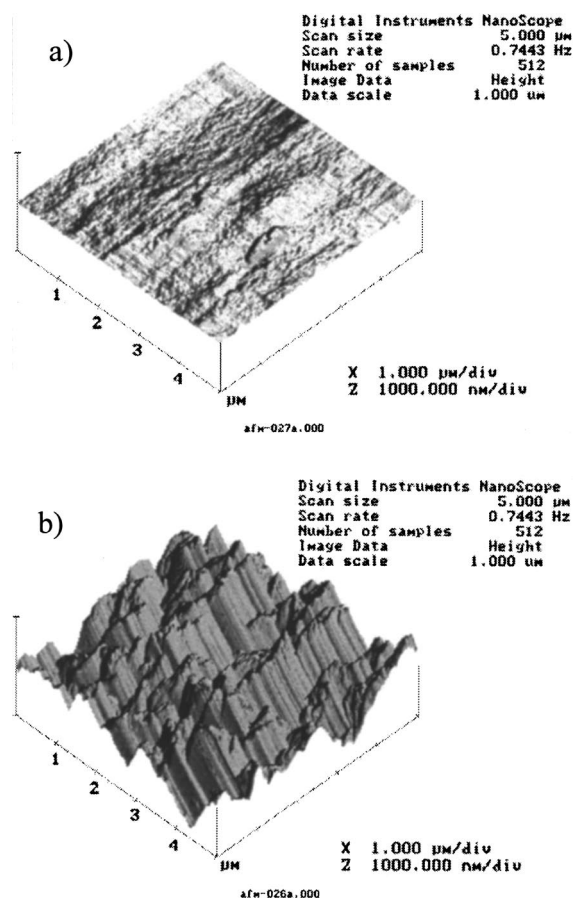


**Figure 1.** AFM images: (a) as-received Nafion 117, (b) ac plasma roughened Nafion 117 (potential, 1350 V; current, 11 mA; duration, 10 min). Scale:  $1.0 \mu\text{m}$  division.



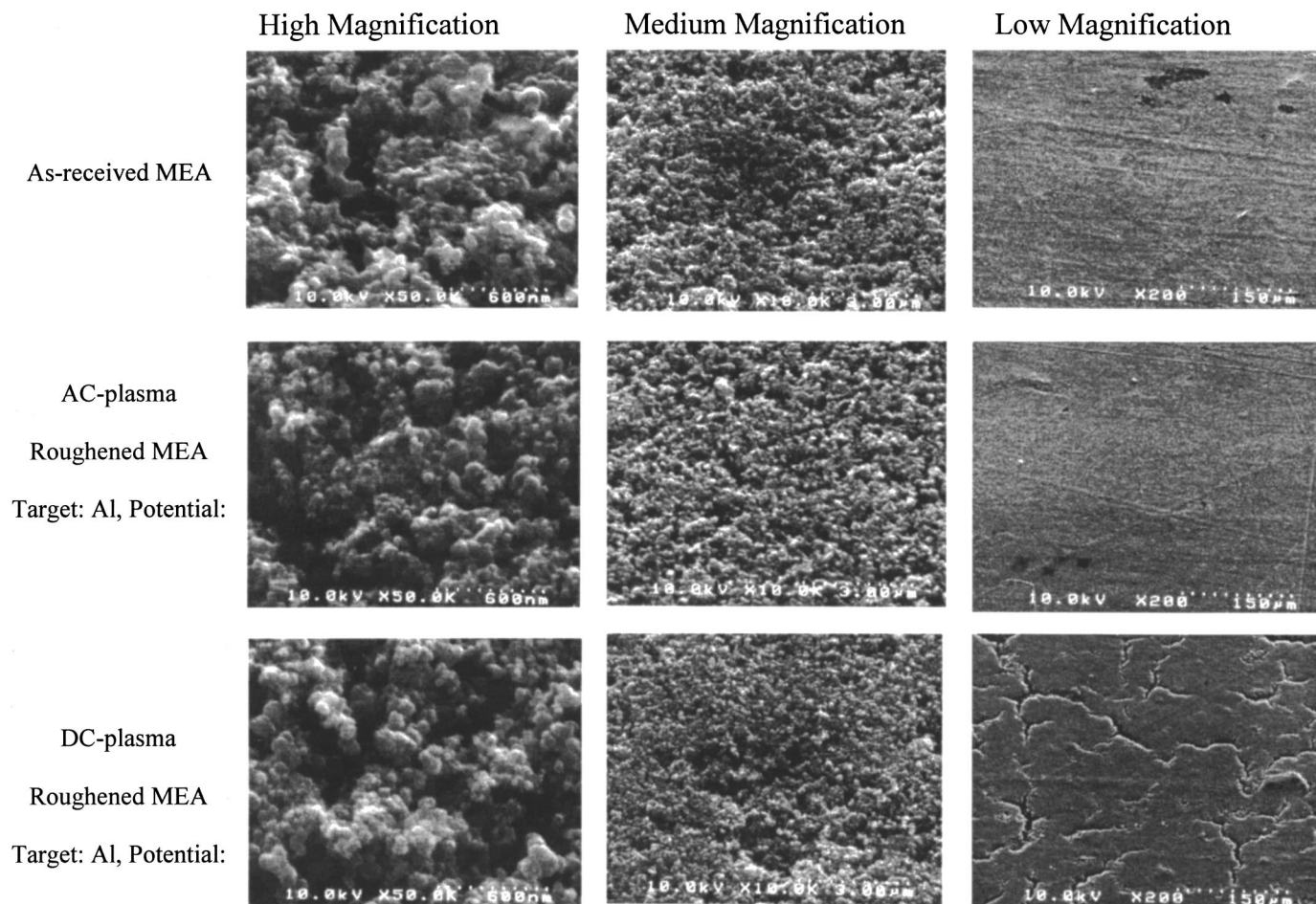


**Figure 2.** SEM images of plasma roughening of MEAs at high (50,000 times), medium (10,000 times), and low (200 times) magnification. The plasma modification had negligible effect on the roughness of the MEA, however, dc roughening tended to crack the surface of the MEA.

~ 65%). Pt did not form continuous films on the  $\text{SiO}_2$  substrate, but rather agglomerated. This is consistent with the literature.<sup>16</sup> The surface coverage was used in conjunction with the bulk density ( $\text{Pt} = 21.4 \text{ g/mL}$ ) and the film thicknesses from the cross-sectional SEM images to calculate the subsequent Pt loadings. Based on this method, the Pt sputter-deposition rate was found to be  $5.6 \mu\text{g Pt/cm}^2/\text{min}$ . Pt loading analyses of all sputtered PEMs, GDLs, and MEAs from Adirondack Environmental Services on yielded Pt loadings that were generally consistent with the deposition rate determined from cross-sectional and top view SEM images.

This sputter deposition rate ( $\mu\text{g/cm}^2/\text{min}$ ) for Pt was found to be constant with respect to time for durations of 5 min or more. The cross-sectional view in Fig. 3 shows that the thickness of 30 and 45 min sputter-deposited Pt is roughly two and three times the thickness of a 15 min deposition of Pt, respectively. Semiquantitative analyses via energy dispersive X-ray spectroscopy (EDXS) and Rutherford backscattering spectrometry (RBS) confirm these Pt deposition rates. These methods in combination with the analysis provided by Adirondack Environmental Services were also used to determine loadings of individual MEUs composed of Pt sputter-deposited layers of less than 5 min duration.

**Sputter-deposition augmentation and addition.**—The sputter deposition treatments performed for this experiment are listed in Table II.

Pt was sputter-deposited on GDLs, PEMs, and MEAs. Figure 4 compares the cell performance of MEUs made from GDLs upon which 15, 30, 45, and 90 min of Pt was sputter deposited as a single layer. In all cases, the equivalent amounts of Pt were added to the

anode and cathode. The MEU comprised of 30 min of sputter-deposited Pt is closest to the baseline MEU in loading ( $0.168$  and  $0.150 \text{ mg Pt/cm}^2$ , respectively). Under conditions of hydrogen/air (anode/cathode) feed at  $70^\circ\text{C}$  and  $1 \text{ atm}$ ,  $15 \text{ min Pt}$  ( $0.084 \text{ mg/cm}^2$ ) deposited on the anode and cathode GDL,  $0.147 \text{ A/cm}^2$  was observed at  $0.6 \text{ V}$  compared to  $0.276 \text{ A/cm}^2$  for the baseline. Doubling the sputter-deposition time to 30 min resulted in a cell performance comparable to the baseline MEA. Figure 4 shows that further amounts of sputter-deposited Pt showed no appreciable increase in cell performance.

The goal of the sputter depositing an additional layer of Pt on the surface of the anode and cathode of the baseline MEA is to increase the performance of the electrodes (primarily the cathode). Oxygen kinetics (at high potentials) and oxygen diffusion (low potentials) are two factors that limit the performance of the fuel cell. It was hoped that the application of this additional Pt layer would increase the rate of the oxygen reduction (by having more available sites) and that by having a layer of Pt on the surface of the MEA, that there would be less diffusional resistances as oxygen would not have to diffuse far to get to a reaction site. Figure 5 compares the cell performance of a baseline MEA to those onto which Pt has been sputter deposited. Under conditions of hydrogen/air feed at  $70^\circ\text{C}$  and  $1 \text{ atm}$ ,  $15 \text{ min of Pt}$  ( $0.84 \text{ mg/cm}^2$ ) deposited on the anode and cathode of a baseline MEA provides an increase in performance at high voltages (from  $0.025$  to  $0.072 \text{ mg/cm}^2$  at  $0.8 \text{ V}$ ). However, the added sputter-deposited layer of Pt clearly reduced the limit at which the gases (oxygen, hydrogen, water vapor) could diffuse through the electrodes. This effect resulted in a reduction in performance of 52%

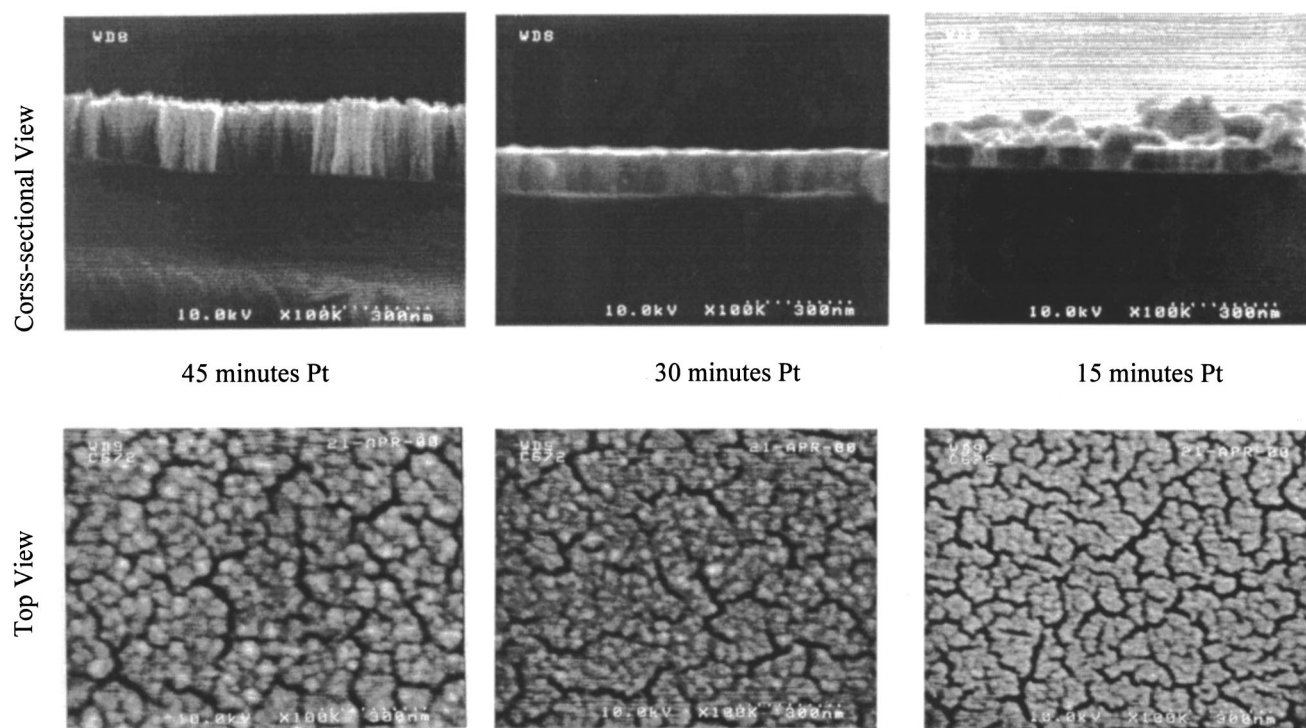


**Figure 3.** Top and cross-sectional SEM images (100,000 times) of sputter-deposited Pt on Si/SiO<sub>2</sub> substrates. Scale: 300 nm (such that the thickness of the 45 min deposition is 200 nm).

**Table II. Sputter-deposition treatments. All Pt depositions were performed identically on the anode and cathode. In the case of a sputter-deposition on a GDL substrate, identical depositions were performed on two GDLs that would then form the anode and cathode.**

Substrate	Addition
MEA (baseline)	15 min sputter-deposited Pt
MEA (baseline)	30 min sputter-deposited Pt
Nafion 117	15 min sputter-deposited Pt
Nafion 117	30 min sputter-deposited Pt
Nafion 117	15 min sputter-deposited Pt + NCI
Nafion 117	30 min sputter-deposited Pt + NCI
GDL	15 min sputter-deposited Pt
GDL	30 min sputter-deposited Pt
GDL	45 min sputter-deposited Pt
GDL	60 min sputter-deposited Pt
GDL	90 min sputter-deposited Pt
GDL	NCI + (5 min sputter-deposited Pt + NCI) × 3
Nafion 117	NCI + (15 min sputter-deposited Pt + NCI) × 3
Nafion 117	NCI + (5 min sputter-deposited Pt + NCI) × 3
Nafion 117	NCI + (2.5 min sputter-deposited Pt + NCI) × 3
Nafion 117	NCI + (1.0 min sputter-deposited Pt + NCI) × 3
Nafion 117	NCI + (0.5 min sputter-deposited Pt + NCI) × 3
Nafion 117	NCI + (0.5 min sputter-deposited Pt + NCI) × 6
Nafion 117	NCI + (0.5 min sputter-deposited Pt + diluted NCI) × 6

at 0.4 V (from 0.56 A/cm<sup>2</sup> to 0.27 cm<sup>2</sup>) for the case where a 15 min (0.084 mg/cm<sup>2</sup>) Pt layer is added to the anode and cathode. Gas diffusion is all but stopped in the case where 30 min of Pt is deposited on top of the baseline MEA, and the result is negligible cell performance. This lack of performance is accompanied by an increase in cell resistance from 25 to 200 mΩ as shown in Table III. It is likely that the resistance is ionic in nature, as the coating of the

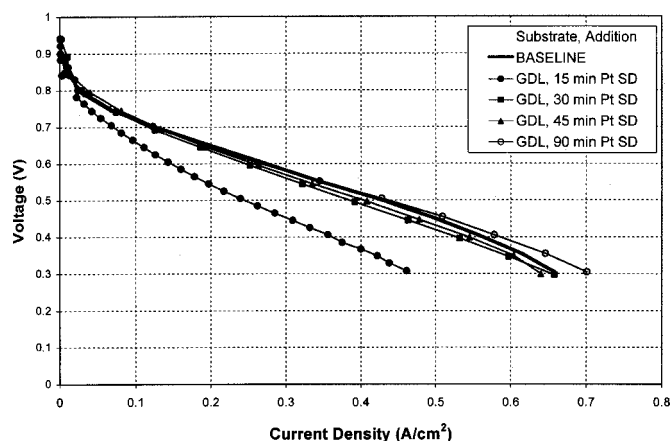


**Figure 4.** Performance comparison for MEUs prepared from GDLs with various sputter-deposited Pt loadings.  $P = 1$  atm,  $T = 70^\circ\text{C}$ .

surface of the MEA fills the pores necessary for the transport of water through to the membrane resulting in a reduction in proton conductivity.

The sputter deposition of Pt onto a Nafion 117 substrate yielded an MEU that showed very poor performance as shown in Fig. 6. Under conditions of hydrogen/air (anode/cathode) feed at 70 C and 1 atm, 15 and 30 min of sputter-deposited Pt deposited on the anode and cathode side of Nafion 117 resulted in current densities of 0.044 and 0.065 A/cm<sup>2</sup> at 0.6 V, respectively. The resistance of the cell at open-circuit voltage was very high compared to the baseline (250 vs. 25 mΩ). In contrast to the sputter-deposition augmented MEAs, it is believed that the high resistance is the result of poor electrical conduction between the catalytic Pt sites and the cathode. As shown in Fig. 3, Pt is not deposited as a continuous film, but an agglomeration



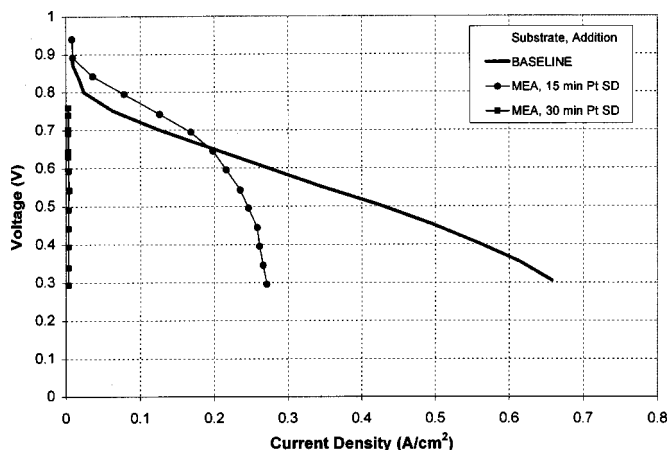


**Figure 5.** Performance comparison of baseline MEAs onto which various amounts of Pt has been sputter deposited.  $P = 1$  atm,  $T = 70^\circ\text{C}$ .

**Table III.** Cell resistance of various MEUs at open-circuit voltage. Resistances were measured by a micrometer set at 1 kHz ac voltage.

Substrate	Addition	Resistance $\epsilon$ (m $\Omega$ )
Baseline	—	25
Baseline	15 min Pt SD	27
Baseline	30 min Pt SD	200
Nafion membrane	15 min Pt SD	250
Nafion membrane	15 min SD + NCI	40
Nafion membrane	30 min Pt SD	83
Nafion membrane	30 min Pt SD + NCI	54
Nafion membrane	NCI + 3 $\times$ (5 min Pt SD + NCI)	27
GDL	15 min Pt SD	21
GDL	30 min Pt SD	23
Baseline	Ru filter (ink-based)	31

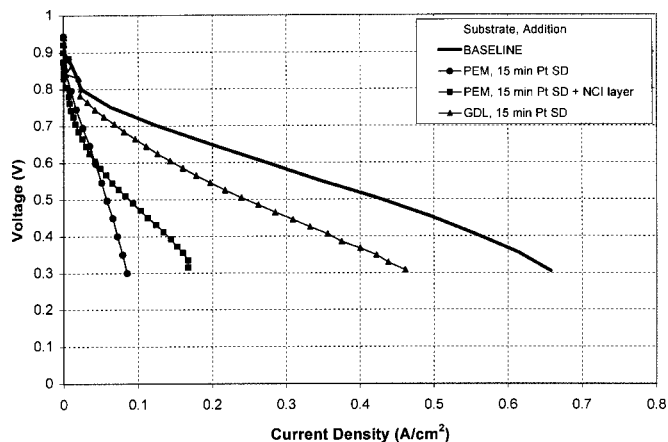


**Figure 6.** Performance comparison of MEUs prepared from PEMs and GDLs with one or several layers of sputter-deposited Pt.  $P = 1$  atm,  $T = 70^\circ\text{C}$ .

of Pt islands with a columnar microstructure. The addition of a layer of NCI (50% Nafion solids by weight) over the layer of sputter-deposited Pt decreases cell resistance and increases performance. Islands of sputter-deposited Pt are connected by the carbon in the NCI, activating the sites by providing a pathway for electrons to flow to and from the sites. In the case of a 15 min Pt deposited on

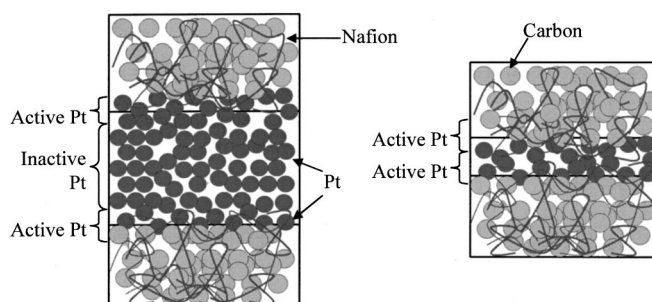


**Figure 7.** Representation of a single layer of a high (left) and low (right) amount of sputter-deposited Pt between layers of Nafion-carbon ink (NCI).

Nafion, Table III shows the drop in resistance from 250 to 40 m $\Omega$  with the addition of the NCI layer, while Fig. 6 shows that there is some improvement in cell performance at lower voltages (0.137 vs. 0.074 A/cm $^2$  at 0.4 V). The Pt islands not in contact with the GDL provide no conduit for the electrons and are thus deactivated.

For an equal amount of sputter-deposited Pt, performance of the resultant MEU was better when applied to the GDL as opposed to the MEA or PEM. The sputter deposition of Pt directly on the membrane showed far less performance (0.044 vs. 0.138 A/cm $^2$  at 0.6 V) than when deposited on the GDL. The rough surface of the GDL allows for the generation of a greater Pt active area. Also the high porosity of the GDL allows gas diffusion to and from the electrodes even after Pt deposition. It is hypothesized that the deposition of a single Pt layer creates regions of active and inactive Pt as shown in the schematic in Fig. 7. Pt is only active as a catalyst when it is in contact with the electrolyte and a conductive support. Pt not in contact with Nafion is inactive because proton transport is not possible. The inherent roughness of the GDL increases this area of active Pt compared to the relative smoothness of the MEA and bare membrane. Even on the GDL the deposition of Pt beyond a given amount (30 min or 0.168 mg/cm $^2$ ) provides no added performance, because the added Pt serves only to increase the layer of inactive Pt described in Fig. 7.

A multilayer electrode technique<sup>14</sup> was used to increase the regions of active Pt area by increasing the number of layers of sputter-deposited Pt. MEAs were prepared from PEMs with multiple layers of sputter-deposited Pt and spray-deposited NCI as shown in Fig. 8. The anode and cathode were built in an identical manner. Figure 9 compares the performance of cells for which the anode and cathode is composed of three sputter-deposited Pt layers dispersed between NCI. Individual Pt layer thicknesses of 15, 5, 2.5, 1.0, and 0.5 min resulted in electrode loadings of 0.2089, 0.07, 0.0795, 0.0407, and 0.027 mg Pt/cm $^2$ , respectively. As the thickness of each layer and resultant Pt loading decreases, the cell performance remains constant. This verifies the theory that the fraction of inactive Pt shown

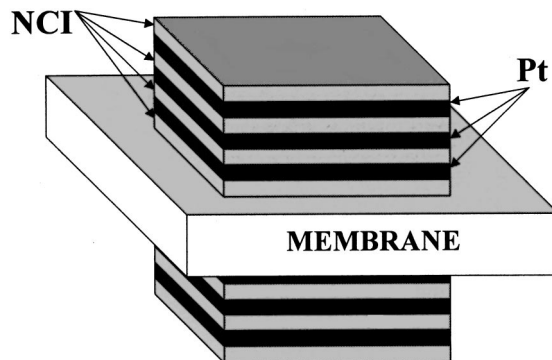


**Figure 8.** Representation of a three layer Pt-NCI MEA.

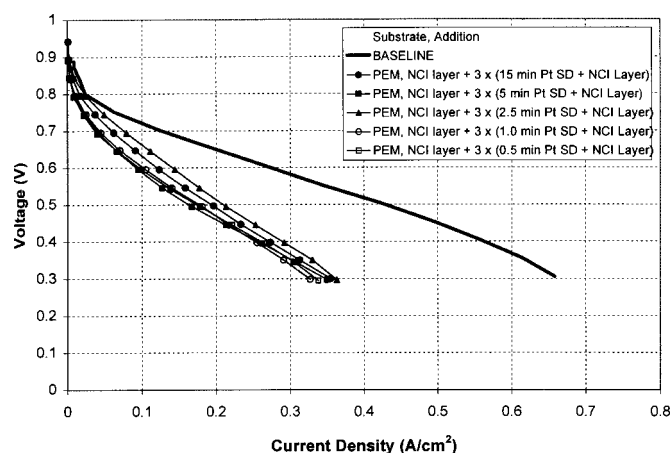


**Figure 9.** Performance comparison between the baseline and three-layer MEAs using various Pt loadings.  $P = 1$  atm,  $T = 70^\circ\text{C}$ . Individual Pt layer thicknesses of 15, 5, 2.5, 1.0, and 0.5 min resulted in electrode loadings of 0.2089, 0.07, 0.0795, 0.0407, 0.027 mg Pt/cm<sup>2</sup>, respectively.

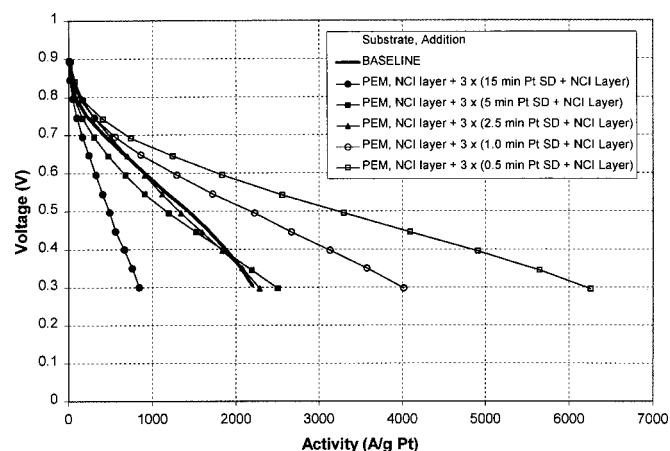


**Figure 10.** Comparison Pt Activity between the baseline and various three-layer anode and cathode MEAs.  $P = 1$  atm,  $T = 70^\circ\text{C}$ .

in Fig. 7 is eliminated as the thickness of each Pt layer is reduced. The amount of active Pt in the three-layer electrode did not change with the thickness of each sputter-deposited layer. Furthermore, all three-layer MEAs outperformed the single Pt layer MEA (0.091–0.140 vs. 0.044 A/cm<sup>2</sup> at 0.6 V), suggesting that using multiple layers increased the active Pt area available for reaction.

Figure 10 shows that fuel cell activity continuously increases as the amount of sputter-deposited Pt in each of the multiple layers is reduced. At 0.6 V, the activity of the 0.5 min Pt/layer MEU is 1835 A/g Pt vs. 905 A/g Pt for the baseline MEA and 670 A/g Pt for the 15 min Pt on the GDL. Even higher activity should be attainable, since a sputter-deposited Pt layer only a few monolayers thick could provide an equivalent number of active catalytic sites (a 0.5 min sputter-deposited layer of Pt is roughly equivalent to six monolayers).

Multilayer treatments were of no benefit when applied to the GDLs as shown in Fig. 11. This is consistent with the high degree of roughness and porosity of the GDL. A high surface area allows successful distribution of sputter-deposited Pt throughout the GDL. As a result, the performance of the single 15 min sputter-deposited layer of Pt on the GDL is greater than an equivalent amount of Pt deposited directly on the membrane in three layers (0.147 vs. 0.091 A/cm<sup>2</sup> at 0.6 V).

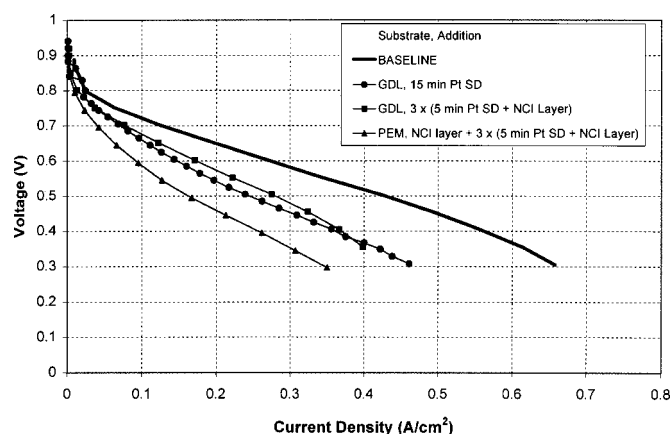


**Figure 11.** Performance comparison of layered PEM and GDL electrodes.  $P = 1$  atm,  $T = 70^\circ\text{C}$ .

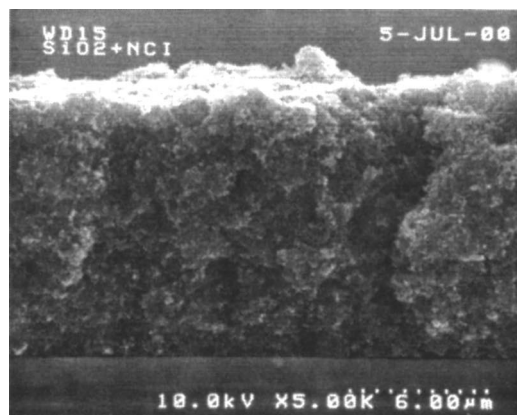
To determine the effect of layering on the performance of the MEA when the layers are applied to the membrane, three different layered catalyst structures were fabricated: (1) an anode and cathode consisting of NCI + (1 min of sputter-deposited Pt + NCI)  $\times$  3; (2) an anode and cathode consisting of NCI + (0.5 min of sputter-deposited Pt + NCI)  $\times$  6; and (3) an anode and cathode consisting of NCI + (0.5 min of sputter-deposited Pt + NCI diluted 1:5 with isopropanol)  $\times$  6.

MEA 2 contains the same amount of Pt as MEA 1, but MEA 2 contains twice the amount of Pt-NCI interfaces as a result of doubling the number of Pt layers from three to six. Comparing the performances of the single-layer 15 min sputtered MEA shown in Fig. 6 and the three-layer sputtered MEAs shown in Fig. 9, the active area and hence cell performance is a function of the number of sputtered layers and not the amount of Pt. Therefore, MEA 2 has roughly double the active area of MEA 1. MEA 3 contains the same number of Pt layers as 2, but the NCI used in 3 is diluted in order to reduce the thickness of the NCI region between each Pt layer. Figure 12a shows a cross-sectional view SEM image of a spray-deposited NCI layer on an SiO<sub>2</sub> substrate. The spray deposited NCI layer is  $\sim$ 12  $\mu\text{m}$  thick. Therefore for MEA 2, the anode and cathode stacks are roughly  $\sim$ 70  $\mu\text{m}$  thick (the thickness of the Pt is negligible). This is much thicker than the anode and cathode of the baseline MEU, which are typically 5–10  $\mu\text{m}$  thick. Like the layers of sputter-deposited Pt, it is not necessary for the NCI layers to be so thick. Based on the fact that a layer of 15 min of sputter-deposited layer is 75 nm thick (see Fig. 3), that the 0.5 min sputter-deposited layer of Pt is a fraction of the thickness of the 15 min layer, and that the NCI layer is roughly 12  $\mu\text{m}$  thick, it can be concluded that the NCI comprises at least 99.9% of the thickness of the multilayer electrodes.

To reduce the thickness of the NCI layers and thus reduce these resistance losses, the NCI was diluted with isopropanol. The thickness of a spray-deposited layer of NCI diluted 1:1 by volume with isopropanol, shown in Fig. 12b, is roughly  $\sim$ 4  $\mu\text{m}$  thick, compared to the 12  $\mu\text{m}$  thickness of the pure NCI. To achieve a multilayered electrode of less than 10  $\mu\text{m}$  (MEA 3), a dilution of 1:5 NCI to isopropanol was used.

Figure 13 shows that as the number of electrode layers is increased from three (MEA 1) to six (MEA 2), the cell performance increases (0.105 to 0.132 A/cm<sup>2</sup> at 0.6 V). However, there is not a doubling of performance that accompanies the doubling of the active area. The increased diffusional, ionic, and electronic resistances caused by the increased thickness of the electrodes of MEA 2 vs. MEA 1 are likely causes for the limited performance increase seen in Fig. 13. Versus the three-layer electrode, gases, protons, and electrons must travel further in the six-layer electrode to get to and from all available Pt sites.





a) Pure NCI



b) Diluted NCI

**Figure 12.** Cross-sectional view SEM images of coating produced by (a) pure NCI, (b) diluted NCI (1:1 by volume with isopropanol).

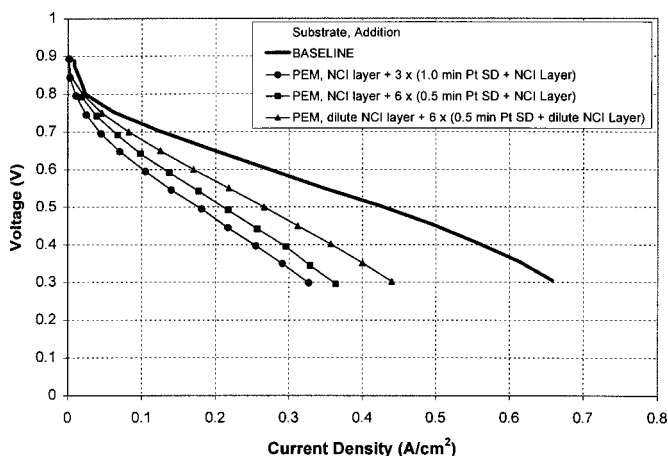


**Figure 13.** Performance comparison of MEAs comprised of three and six layers (anode and cathode) using pure NCI.  $P = 1$  atm,  $T = 70^\circ\text{C}$ .

As shown in Fig. 13, MEA 3 outperforms MEA 2 0.170 to 0.132  $\text{A}/\text{cm}^2$  at 0.6 V. This value is closer to double that of MEA 1, containing three-layer electrodes. This further emphasizes the fact that as the thickness of the NCI decreases, performance increases. The performance of MEA 3 is also greater than the MEU containing 15 min of Pt was sputtered onto the anode and cathode GDL, but

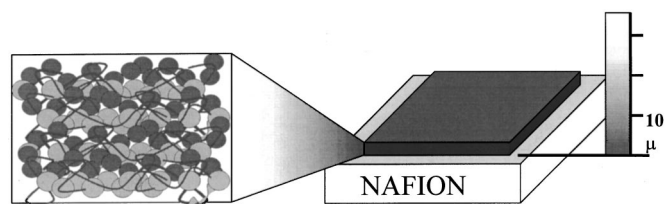


**Figure 14.** Representation of a continuous three-phase interface (Nafion, carbon, catalyst) prepared by applying Nafion, carbon, and Pt simultaneously.

less than the MEU containing 30 min of Pt on the anode and cathode GDL and less than the performance of the baseline MEA. The loading for each electrode for the MEA 3 was found to be  $\sim 0.0324$  mg  $\text{Pt}/\text{cm}^2$  anode/cathode (0.0648 mg  $\text{Pt}/\text{cm}^2$  in the entire MEA) resulting in an activity of 2650  $\text{A}/\text{g}$  Pt at 0.6 V, the highest value of all MEAs tested and three times greater than the baseline (905  $\text{A}/\text{g}$ ).

### Conclusions

1. Of the three substrates studied (membrane, GDL, and MEA), sputter-depositing Pt on the GDL showed the best performance, equaling that of the baseline MEA for an equivalent amount of Pt. However, sputter-depositing multiple layers of Pt on the GDL showed no improvement in performance over an equivalent amount of Pt sputtered as a single layer.

2. MEAs built from multilayered sputter-deposited Pt and spray-deposited NCI demonstrated improved performance over single-layer, sputter-deposited MEAs of equivalent or greater Pt loadings. By reducing the amount of Pt and NCI in each layer, a level of Pt activity higher than that of the baseline has been achieved. This level of activity is maintained as the number of layers increase from three to six, provided the NCI layers are sufficiently thin. The preparation of MEAs with extremely high activity suggests future study. This is hypothesized to be the result of increasing the three phases of Pt, Nafion, and carbon necessary for an active catalyst.

3. The optimal performance achieved from the MEA containing six-layer Pt + dilute NCI anode and cathode was 0.17  $\text{A}/\text{cm}^2$  at 0.6 V. This is less than the performance achieved by Cha and Lee (roughly 0.32  $\text{A}/\text{cm}^2$  at 0.6 V). However, all fuel cells in this experiment were fed  $\text{H}_2/\text{air}$  at 1 atm and  $70^\circ\text{C}$ , compared to an  $\text{H}_2/\text{O}_2$  feed at 1 atm and  $60^\circ\text{C}$  used by Cha and Lee.<sup>14</sup>

4. Catalyst activities of greater than 2650  $\text{A}/\text{g}$  were achieved at 0.6 V and 5500  $\text{A}/\text{g}$  at 0.4 V from the MEA containing six-layer Pt + dilute NCI anode and cathode.

5. Further research can be done to optimize this three-phase interface area and eliminate the unused portion of the electrode. Even diluting the NCI between each sputter-deposited layer 5:1 with isopropanol results in a catalyst electrode in which NCI accounts for 99% of the width. However, to generate an electrode with even more than six Pt + NCI layers is neither the most economical (due to the time required to generate such a multilayered MEA) nor most effective approach. The generation of a continuous three-phase interface is the ultimate goal of this method, and this is what should be pursued using the method of sputter deposition. Simultaneously sputter-depositing Pt and spray-depositing NCI could produce a continuous three-phase interface region such as that shown in Fig. 14. This would result in an extremely thin ( $\sim 1$  micrometer) electrode that is conceptually almost identical to the ink-based catalyst electrode used in the baseline. The only difference is that the particle size of the sputter-deposited Pt would be much smaller, resulting in greater Pt surface area, higher Pt activity, higher Pt utilization, and hence a superior performing electrode compared to a conventional electrode prepared from colloidal catalyst inks. Also by applying this Pt/C/Nafion electrode in a single application to the proton-exchange membrane, the process is less time consuming and, thus, more economical.

### Acknowledgments

The authors acknowledge the financial support from the National Institute of Standards and Technology under cooperative agreement no. 70NANB8H4039.

University of South Carolina assisted in meeting the publication costs of this article.

### References

1. Arthur D. Little Inc., *Cost Analysis of Fuel Cell Systems for Transportation: Baseline System Cost Estimate*, Final Report to Department of Energy (2000).
2. Solicitation for Financial Assistance Applications (SFAA) no. DE-RP04-01AL67057 Research and Development and Analysis for Energy Efficient Technologies in Transportation and Buildings Applications, Nov 21, 2000.
3. E. A. Ticianelli, C. R. Derouin, and S. Srinivasan, *J. Electroanal. Chem.*, **251**, 275 (1988).
4. M. S. Wilson. U.S. Pat. 5,211,984 (1993).
5. V. A. Paganin, E. A. Ticianelli, and E. R. Gonzalez, in *Proton Conducting Fuel Cells I*, S. Gottesfeld, G. Halpert, and A. Landgrebe, Editors, PV 95-23, p. 102, The Electrochemical Society Proceedings Series, Pennington, NJ (1995).
6. C. K. Witham, W. Chun, T. I. Valdez, and S. R. Narayanan, *Electrochem. Solid-State Lett.*, **3**, 497 (2000).
7. E. J. Taylor, E. B. Anderson, and N. R. K. Vilambi, *J. Electrochem. Soc.*, **139**, L45 (1992).
8. K. H. Choi, H. S. Kim, and T. H. Lee, *J. Power Sources*, **75**, 230 (1998).
9. S. Srinivasan, D. J. Manko, J. Koch, M. A. Enayetullah, and A. J. Appleby, *J. Power Sources*, **29**, 367 (1990).
10. E. A. Ticianelli, C. R. Derouin, A. Redondo, and S. Srinivasan, *J. Electrochem. Soc.*, **135**, 2209 (1988).
11. S. Mukerjee, S. Srinivasan, and A. J. Appleby, *Electrochim. Acta*, **38**, 1661 (1993).
12. S. Hirano, J. Kim, and S. Srinivasan, *Electrochim. Acta*, **42**, 1587 (1997).
13. C. K. Witham, W. Chun, T. I. Valdez, and S. R. Narayanan, *Electrochem. Solid-State Lett.*, **3**, 497 (2000).
14. S. Y. Cha and W. M. Lee, *J. Electrochem. Soc.*, **146**, 4055 (1999).
15. J. A. Thornton, *Deposition Technologies for Films and Coatings*, p. 170, Noyes Publications, Park Ridge, NJ (1982).
16. J. A. Poirier and G. E. Stoner, *J. Electrochem. Soc.*, **141**, 425 (1994).